Variation in anthelmintic responses are driven by genetic differences among diverse *C. elegans* wild strains

Amanda O. Shaver[1], Janneke Wit[1], Clayton M. Dilks[1], Timothy A. Crombie[1], Hanchen Li[2], Raffi V. Aroian[2], Erik C. Andersen[1]

Affiliations:

[1] Molecular Biosciences, Northwestern University, Evanston, Illinois, United States of America
[2] Program in Molecular Medicine, University of Massachusetts Medical School, Worcester, Massachusetts, United States of America

Corresponding author:
Erik C. Andersen
Department of Molecular Biosciences
Northwestern University
4619 Silverman Hall
2205 Tech Drive
Evanston, IL 60208
847-467-4382
erik.andersen@gmail.com

Short Title: Genetic differences in *C. elegans* anthelmintic responses

Keywords: Anthelmintic drugs, *C. elegans*, Dose responses, Natural variation

ORCIDs and emails:
Amanda O. Shaver: 0000-0002-2910-1505, amanda.shaver@northwestern.edu
Janneke Wit: 0000-0002-3116-744X, jannekewit@gmail.com
Clayton M. Dilks: 0000-0002-4622-8460, claydilks@yahoo.com
Timothy A. Crombie: 0000-0002-5645-4154, tcrombie@northwestern.edu
Raffi V. Aroian, 0000-0002-9741-3834, raffi.aroian@umassmed.edu
Erik C. Andersen: 0000-0003-0229-9651, erik.andersen@northwestern.edu, erik.andersen@gmail.com

Journal: *PLOS Pathogens*

37 **GRAPHICAL ABSTRACT**

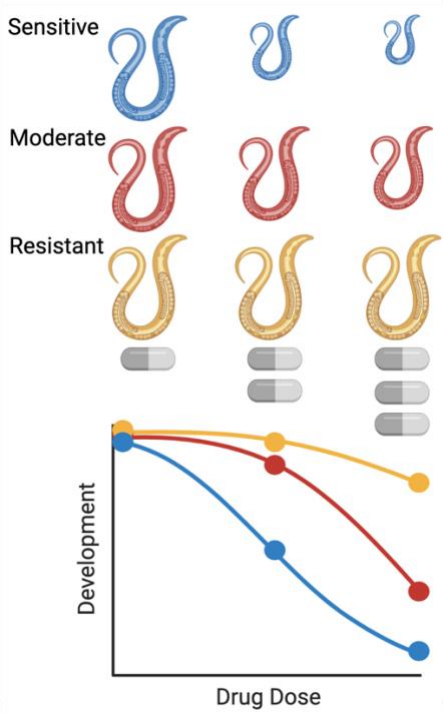

ABSTRACT

Treatment of parasitic nematode infections in humans and livestock relies on a small arsenal of anthelmintic drugs that have historically reduced parasite burdens. However, anthelmintic resistance (AR) is increasing, and little is known about the molecular and genetic causes of resistance for most drugs. The free-living roundworm *Caenorhabditis elegans* has proven to be a tractable model to understand AR, where studies have led to the identification of molecular targets of all major anthelmintic drug classes. Here, we used genetically diverse *C. elegans* strains to perform dose-response analyses across 26 anthelmintic drugs that represent the three major anthelmintic drug classes (benzimidazoles, macrocyclic lactones, and nicotinic acetylcholine receptor agonists) in addition to seven other anthelmintic classes. First, we found that *C. elegans* strains displayed significant variation in anthelmintic responses across drug classes. Dose-response trends within a drug class showed that the *C. elegans* strains elicited similar responses within the benzimidazoles but variable responses in the macrocyclic lactones and nicotinic acetylcholine receptor agonists. Next, we compared the effective concentration estimates to induce a 10% maximal response (EC_{10}) and slope estimates of each dose-response curve of each strain to the reference strain, N2, which enabled the identification of anthelmintics with population-wide differences to understand how genetics contribute to AR. Because genetically diverse strains displayed differential susceptibilities within and across anthelmintics, we show that *C. elegans* is a useful model for screening potential nematicides. Third, we quantified the heritability of responses to each anthelmintic and observed a significant correlation between exposure closest to the EC_{10} and the exposure that exhibited the most heritable responses. Heritable genetic variation can be explained by strain-specific anthelmintic responses within and across drug classes. These results suggest drugs to prioritize in genome-wide association studies, which will enable the identification of AR genes.

AUTHOR SUMMARY

Parasitic nematodes infect most animal species and significantly impact human and animal health. Control of parasitic nematodes in host species relies on a limited collection of anthelmintic drugs. However, anthelmintic resistance is widespread, which threatens our ability to control parasitic nematode populations. Here, we used the non-parasitic roundworm *Caenorhabditis elegans* as a model to study anthelmintic resistance across 26 anthelmintics that span ten drug classes. We leveraged the genetic diversity of *C. elegans* to quantify anthelmintic responses across a range of doses, estimate dose-response curves, fit strain-specific model parameters, and calculate the contributions of genetics to these parameters. We found that genetic variation within a species plays a considerable role in anthelmintic responses within and across drug classes. Our results emphasize how the incorporation of genetically diverse *C. elegans* strains is necessary to understand anthelmintic response variation found in natural populations. These results highlight drugs to prioritize in future mapping studies to identify genes involved in anthelmintic resistance.

INTRODUCTION

Parasitic nematodes are incredibly diverse and infect most animal and plant species [1,2]. Treatments rely on a limited arsenal of anthelmintic drugs with the same drug classes used across most parasite species [3]. The three major anthelmintic classes are benzimidazoles (BZs), macrocyclic lactones (MLs), and nicotinic acetylcholine receptor (nAChR) agonists. Over-reliance and inappropriate use of these anthelmintics have placed strong selective pressures on parasites and caused the evolution of anthelmintic resistance (AR) in every drug class [3]. Over time, AR causes the drug to become ineffective [4]. In many cases, AR is highly heritable, which suggests that natural genetic variants play an important role in the evolution of resistant nematodes [5,6]. With the heavy burden parasitic nematodes place on global health, the limited suite of drugs currently available, and AR on the rise, it is imperative that we identify resistance alleles. With this knowledge, we can responsibly apply drugs and implement treatment strategies to reduce our global infection rate and burden of parasitic nematodes.

Most of what we know about mechanisms of resistance comes from studies of a single strain within a single species, the laboratory-adapted strain of *Caenorhabditis elegans* called N2. However, a single genetic background, whether in a free-living or parasitic species, cannot capture the enormous diversity present in the entire species, nor can it predict how natural populations of parasitic nematodes will respond to a drug [7]. In aggregate, single strains from many species might capture phylum-level variation, which strengthens the opportunity to identify genes involved in mechanisms of resistance. It is difficult to accurately test AR in genetically diverse parasitic nematodes because of multiple factors: a lack of access to relevant life cycle stages, lack of global sample collections, host-dependent and cost-intensive laboratory life cycles, complex or non-existent *in vitro* culture systems, and a limited molecular toolkit [7].

With its ease of growth, genetic tractability, and ample molecular toolkit, the roundworm *C. elegans* is our most useful model to study AR. To date, *C. elegans* has contributed to the

identification and characterization of mechanisms of resistance of all major anthelmintic drug classes [8–14]. Additionally, the natural genetic variation across the *C. elegans* species is accessible and continuously archived in the *C. elegans* Natural Diversity Resource (CeNDR), which has facilitated the characterization of natural responses to anthelmintic drugs [11,15,16]. Whole-genome sequence data and identified AR variants are available for CeNDR strains and can be queried to identify orthologous genes between *C. elegans* and parasites [8]. Lastly, because of the tractability of *C. elegans* and established high-throughput assays (HTA), we can measure *C. elegans* responses to any soluble compound [17]. Thus, the genetic diversity of *C. elegans* can enable the discovery of the molecular targets of anthelmintics, which are likely to translate across parasitic nematode species.

Here, we performed dose-response analyses that used 26 anthelmintics across six genetically diverse *C. elegans* strains to identify how growth rate was affected. The anthelmintics used in this study represent the three major anthelmintic drug classes (BZs, MLs, and nAChR agonists) in addition to seven other classes of anthelmintics (nicotinic acetylcholine receptor [nAChR] antagonists, a pore-forming crystal protein, a cyclicoctadepsipeptide, diethylcarbamazine, piperazine, a salicylanilide, and schistosomicides). We measured nematode development after drug exposure for six genetically diverse *C. elegans* strains using an established high-throughput phenotyping assay [17]. We assayed the strains with high levels of replication, collecting a total of 48,343 replicate anthelmintic responses across genetically diverse *C. elegans* strains, a throughput not possible using parasites. We used phenotypic responses to each anthelmintic to estimate dose-response curves, fit strain-specific model parameters, and calculate the contributions of genetics to these anthelmintic responses. Our results emphasize how the incorporation of natural genetic variation is necessary to quantify drug responses and identify the range of drug susceptibilities in natural populations. Importantly, studies focusing on

125 genetic variation increase the likelihood of identifying orthologous genes between *C. elegans* and
126 parasites of interest and, in turn, discover mechanisms of resistance shared across species [8].
127
128 ## RESULTS AND DISCUSSION
129 ### High-throughput assays across six wild strains facilitated dose-response assessments of
130 ### 26 anthelmintic drugs
131 Dose-response assessments were performed using a microscopy-based high-throughput
132 phenotyping assay for developmental delay in response to 26 anthelmintics (**Fig 1**). Anthelmintics
133 assayed were five different BZs, seven MLs, three nAChR agonists, three nAChR antagonists,
134 one pore-forming crystal toxin, one cyclooctadepsipeptide, one diethylcarbamazine, one
135 pyrazinoisoquinoline, one salicylanilide, and three schistosomicides (**Table 1**). Six genetically
136 diverse *C. elegans* strains were exposed to each anthelmintic in high replication. After measuring
137 nematode responses, phenotypic data were cleaned and processed (see *Methods*). Next, dose-
138 response curves were estimated for each anthelmintic to describe how genetic variation
139 contributed to differences in anthelmintic resistance among strains. Differences in responses were
140 measured by the change in developmental rate, as measured by animal length. Nematodes grow
141 longer over time, and anthelmintics have been shown to slow this development [9,10,18–21].
142 Therefore, shorter animals after drug exposure demonstrated that the anthelmintic had a
143 detrimental effect on development.

144

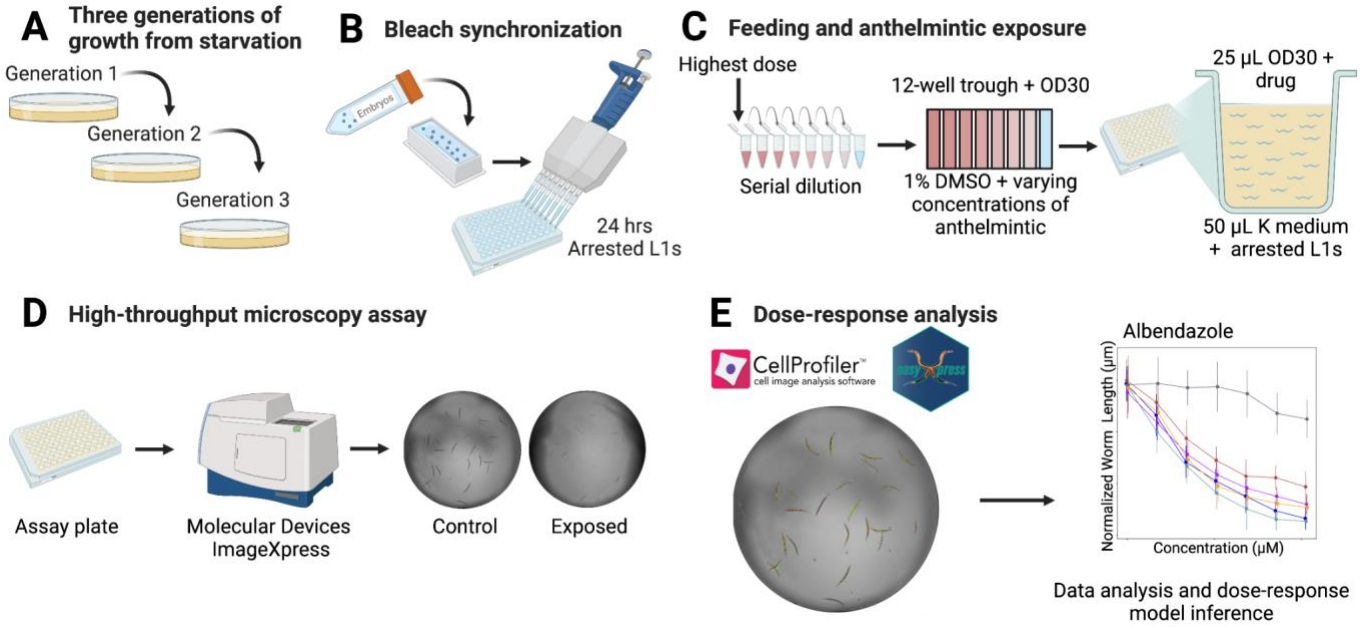

145

146 **Figure 1. The high-throughput phenotyping assay allows for rapid dose-response**
147 **assessments across genetically diverse *C. elegans* strains. A)** strains were passaged for
148 three generations to reduce generational effects of starvation. **B)** strains were bleach
149 synchronized to collect embryos and then hatched and arrested at the L1 larval stage. **C)** Animals
150 were fed and exposed to anthelmintics. **D)** After 48 hours of growth, animals were imaged to
151 collect phenotypic measurements. **E)** Data were cleaned, and dose-response analysis was
152 performed. Detailed descriptions of all steps can be found in *Methods*. Created with
153 BioRender.com. Modified from a previous version [22].

Drug Class	Drug Subclass	Drug
Benzimidazoles (BZ)		Albendazole Benomyl Fenbendazole Mebendazole Thiabendazole
Macrocyclic Lactones (ML)	Avermectins	Abamectin Doramectin Eprinomectin Ivermectin Selamectin
	Milbemycins	Milbemycin oxime Moxidectin
Nicotinic acetylcholine receptor (nAChR) agonists	Imidazothiazoles	Levamisole
	Tetrahydropyrimidines	Morantel citrate Pyrantel citrate
Nicotinic acetylcholine receptor (nAChR) antagonists	Amino-acetonitrile Derivatives (AADs)	Monepantel sulfone LY33414916 Monepantel sulfide LY3348298
	Spiroindoles	Derquantel
Crystal protein		Cry5B
Cyclicoctadepsipeptides		Emodepside
Schistosomicides	1,3-thiazoles	Niridazole
	Quinolines	Oxamniquine
	Praziquantel	Praziquantel
Other	Diethylcarbamazine	Diethylcarbamazine citrate
	Pyrazinoisoquinolines	Piperazine
	Salicylanilides	Closantel

Table 1. Drug class, subclass, and drugs used in this study.

A four-parameter log-logistic dose-response curve was modeled for each of the 26 anthelmintics, where normalized median animal length was used as the metric for a phenotypic response (see *Methods*). For each strain-specific dose-response model, slope (*b*) and effective concentration (*e*) were estimated with strain as a covariate (**S1 Table**, **S2 Table**). EC_{10} estimates were found to be more heritable than half maximal effective concentration (EC_{50}) estimates and were therefore used throughout our analyses (**S1 Fig**). Dose-response relationships described

how different strains were affected at varying levels of anthelmintic exposure providing insights into how genetic differences impact anthelmintic susceptibility.

To test for differences in AR among the strains, we looked for differences in the strain-specific dose-response model parameters. We found differences in EC_{10} values for 22 anthelmintics (**S1 Table**). Next, we focused on EC_{10} comparisons between the reference strain N2 and all other strains (**S3 Table**). In total, we observed 44 instances across 22 compounds where at least one strain was significantly more resistant or sensitive than the reference strain N2 using EC_{10} as a proxy (Student's t-test, Bonferroni correction; $p_{adj} < 0.05$). Because most studies in *C. elegans* AR have been conducted using the laboratory reference strain, N2, or mutant strains in the N2 genetic background, these results emphasize the importance of using genetically diverse individuals to understand drug responses. Furthermore, the observed frequency of strains with significantly greater anthelmintic sensitivity than the N2 strain was different than what is expected under the null expectation (see *Methods*; Fisher exact test; $p < 0.05$), which suggests that diverse *C. elegans* strains are not equally likely to be susceptible or resistant with respect to the commonly used N2 reference strain. The strain MY16 displayed the most sensitivity and resistance compared to the N2 strain, making up 31% and 63% of the cases, respectively.

Out of the 130 strain-specific slope comparisons with respect to the N2 strain, we observed 92 instances across the 26 compounds where a strain had a significantly different slope than the N2 strain (**S4 Table**). However, slope estimate comparisons between the N2 strain and every other strain only describe part of the breadth of *C. elegans* anthelmintic responses. For this reason, we compared all slopes in a pairwise fashion. Out of the 390 total strain-specific slope comparisons, we observed 275 pairwise instances across the 26 compounds where one strain had a significantly different slope than another strain (**S4 Table**). The variation in strain-specific slope comparisons further supports how the incorporation of genetic diversity is necessary to identify anthelmintic responses within a species. Here, we reinforce what previous studies have

188 shown, that *C. elegans* is a powerful model for assessing the impact of genetic differences on
189 phenotypic variation [23].
190
191 **Variation in response to BZs is driven by genetic differences among naturally diverse**
192 **strains**
193 Although BZs are essential in human and veterinary medicine, resistance to this drug class
194 is prominent and common in natural parasite populations [24,25]. Historically, the mechanisms of
195 nematode resistance to BZs were thought to have been limited to variants in the drug target beta-
196 tubulin [26–29]. However, genetic differences in beta-tubulin genes do not explain all intraspecific
197 and interspecific variations observed in BZs efficacy [30] or in responses to different BZs
198 derivatives [31,32]. Genome-wide association studies (GWAS) of responses to albendazole, a
199 widely used BZ, found quantitative trait loci (QTL) that do not overlap with beta-tubulin genes,
200 suggesting that additional genes are involved in albendazole resistance [18]. Additionally,
201 previous work, which included genetically diverse strains of *C. elegans* and
202 *Caenorhabditis briggsae*, a closely related selfing species, found that conserved and drug-
203 specific loci contribute to the effects of BZs (albendazole, fenbendazole, mebendazole, and
204 thiabendazole) [33]. Because of evidence that additional genes beyond beta-tubulin genes are
205 involved in BZs resistance, we have yet to fully understand the mechanisms of BZs resistance.
206 We assessed how natural variation contributes to phenotypic responses across five
207 clinically relevant BZs (albendazole, benomyl, fenbendazole, mebendazole, and thiabendazole)
208 that are widely used in human and veterinary medicine. The panel of six genetically divergent
209 *C. elegans* wild strains was exposed to increasing concentrations of the five BZs (**S5 Table, Fig**
210 **2**). The strain MY16 displayed resistance in all five BZ dose-response curves, where the EC_{10} for
211 MY16 was significantly higher than EC_{10} estimates from all the other strains in every BZ (**Fig 2**).
212 The MY16 strain has a non-synonymous variant in the beta-tubulin gene *ben-1*, causing an amino

acid change (A185P) [34] and a presumptive reduction in *ben-1* function. The other five strains do not have variants known to reduce *ben-1* function.

Benzimidazole strain-specific slope (*b*) estimates for each dose-response model varied but followed similar trends compared to EC_{10} estimates (**Fig 3A**, **Fig 3B**). These results suggest that the genetic differences among *C. elegans* strains mediate differential susceptibility across BZs. To quantify the degree of phenotypic variation attributable to segregating genetic differences among strains, we first estimated broad-sense heritability (H^2) and narrow-sense heritability (h^2) of the phenotypic response for each dose of every BZ (see *Methods*) (**Fig 3C**). For example, we observed that H^2 ranged from 0 in 1 µM albendazole to 0.87 in 51.54 µM albendazole, and h^2 ranged from 0 in 1 µM albendazole to 0.73 in 51.54 µM albendazole. This heritable response indicated that genetic differences among the six strains underlie the variation in albendazole responses. Importantly, all five BZs had highly heritable responses, which indicates that the genetic diversity of *C. elegans* can be used to identify additional molecular mechanisms of BZs resistance beyond the *ben-1* beta-tubulin gene.

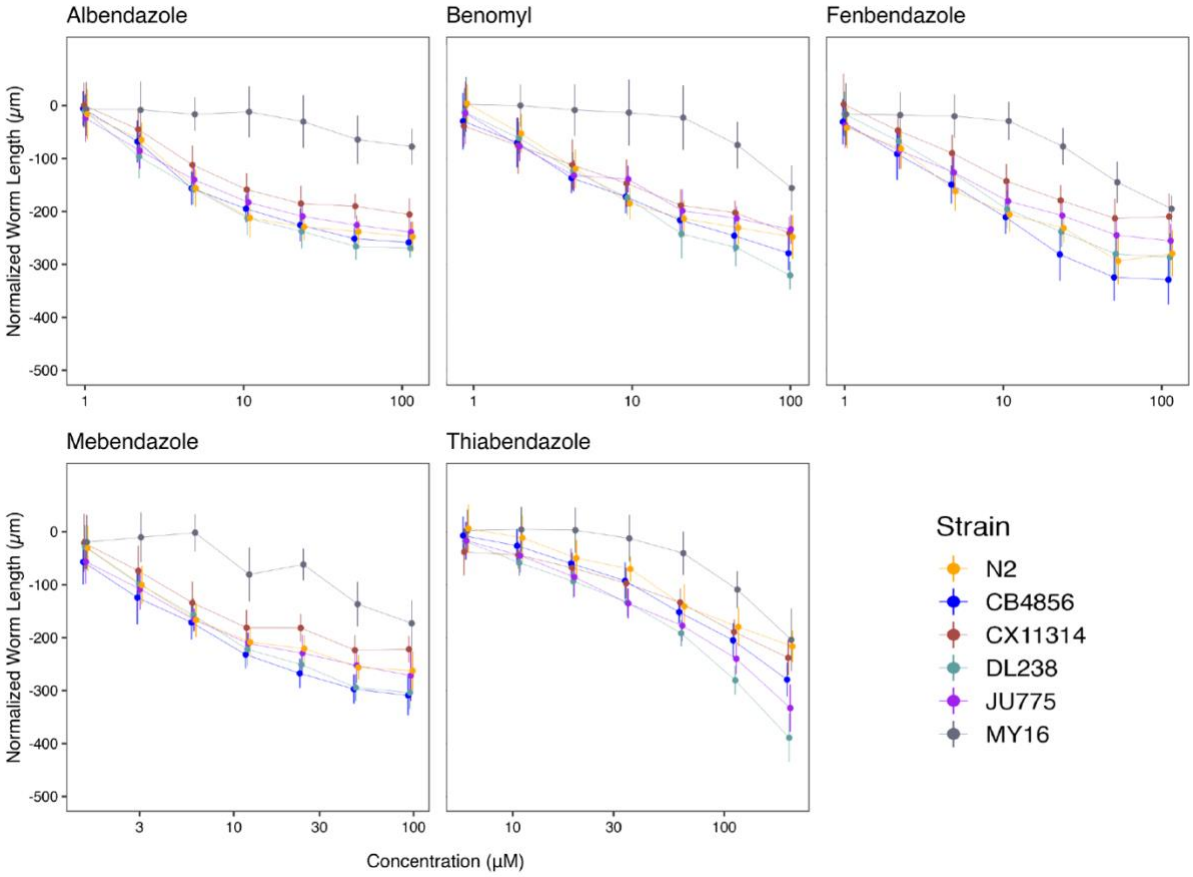

Figure 2. Dose-response curves for benzimidazoles (BZs). Normalized animal lengths (y-axis) are plotted for each strain as a function of the dose of benzimidazole supplied in the high-throughput phenotyping assay (x-axis); Albendazole, Benomyl, Fenbendazole, Mebendazole, and Thiabendazole. Strains are denoted by color. Lines extending vertically from points represent the standard deviation from the mean response. Statistical normalization of animal lengths is described in *Methods*.

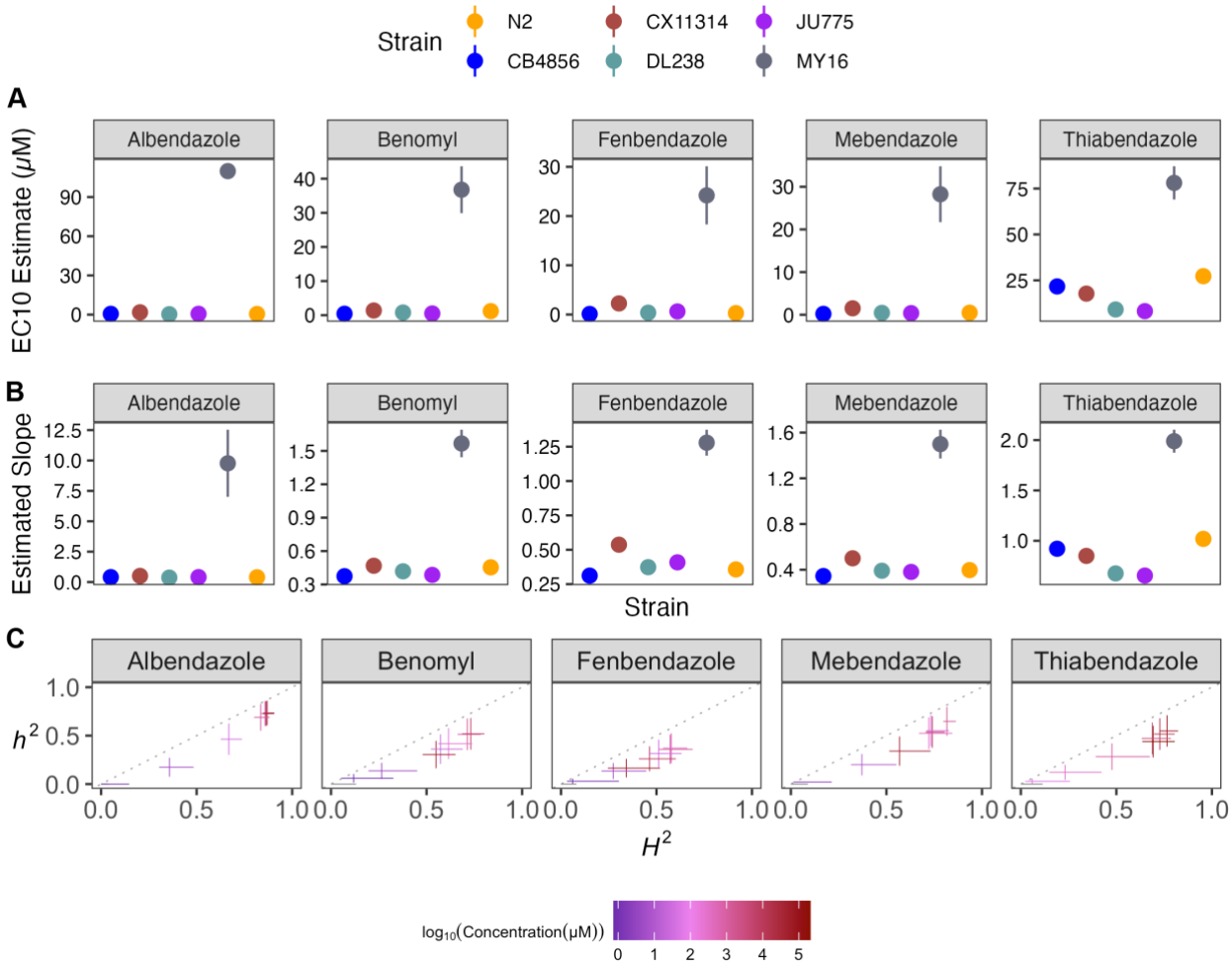

Figure 3. Variation in benzimidazole (BZ) EC_{10} dose-response and slope estimates can be explained by genetic variation across strains. A) Strain-specific EC_{10} estimates (*e*) for each benzimidazole are displayed for each strain. Standard errors for each strain- and anthelmintic-specific EC_{10} estimates are shown. **B)** Strain-specific slope estimates (*b*) for each benzimidazole are displayed for each strain. Standard errors for each strain- and anthelmintic-specific slope estimate are indicated by the line extending vertically from each point. **C)** The broad-sense (x-axis) and narrow-sense heritability (y-axis) of normalized animal length measurements were calculated for each concentration of each benzimidazole (*Methods*; *Broad-sense and narrow-sense heritability calculations*). The color of each cross corresponds to the log-transformed dose for which those calculations were performed. The horizontal line of the cross corresponds to the confidence interval of the broad-sense heritability estimate obtained by bootstrapping, and the vertical line of the cross corresponds to the standard error of the narrow-sense heritability estimate.

Because *ben-1* is not the only gene involved in BZs responses [18,33,35], we removed the MY16 strain from our analyses to observe how smaller genetic effects play a role in BZs

responses in the other five strains (**S2 Fig**). After removing MY16, we observed that the strain CX11314 displayed the greatest resistance among the remaining five strains in all BZs except thiabendazole. The strain N2 displayed the greatest resistance in thiabendazole after MY16. Also, the strains CB4856 and JU775, previously described as sensitive to BZs [34,36], displayed sensitivity across BZs and significant variability in thiabendazole, where the JU775 strain was more sensitive than the CB4856 strain (**S2 Fig**). Even after removing MY16, we found that responses for thiabendazole were highly heritable, although moderately heritable responses were observed for albendazole. Benomyl, fenbendazole, and mebendazole had reduced heritability. These results support the previous findings that *ben-1* is not the only gene involved in BZs resistance and that diverse *C. elegans* strains vary across a spectrum of BZ responses [18,33,35]. The strain MY16 is a striking example of how well natural BZ resistance alleles can protect nematodes from BZ treatment. In the context of natural parasitic nematode populations, it is easy to imagine how such beneficial alleles could spread rapidly and further exacerbate parasitic burdens.

Small variations in MLs dosage can significantly alter drug effectiveness among naturally diverse strains

The MLs comprise avermectins and milbemycins and are an essential class of anthelmintics because of our high dependence on them to control nematode parasites in livestock, companion animals, and humans [37]. Previous genetic screens performed in the *C. elegans* laboratory-adapted reference strain, N2, identified three genes that encode glutamate-gated chloride (GluCl) channel subunits (*glc-1*, *avr-14*, and *avr-15*) that are targeted by MLs [38,39]. Studies of abamectin have found additional loci involved in resistance [36]. By contrast, ML resistant parasitic nematode isolates do not have mutations in genes that encode GluCl channel subunits, suggesting additional mechanisms of resistance to MLs exist [40,41].

Quantitative genetic mappings in free-living and parasitic nematode species have identified genomic regions that confer drug resistance [18,33,36,41–44]. Altogether, mutations in GluCl channel genes have modest effects on some ML responses and do not explain the full spectrum of AR in this class. Other genes must be investigated to understand ML mechanisms of resistance.

Here, we assessed how natural variation contributes to phenotypic responses across seven MLs composed of five avermectins (abamectin, doramectin, eprinomectin, ivermectin, and selamectin) and two milbemycins (milbemycin and moxidectin) (**S5 Table**, **Fig 4**). We observed different susceptibility trends within and across avermectins and milbemycins. We found that the rank order among strains displaying the highest EC_{10} varied among MLs. The strain DL238 had the highest EC_{10} in eprinomectin and milbemycin. The strains CB4856 and N2 displayed the highest EC_{10} in doramectin. The N2 strain displayed the highest EC_{10} in selamectin (**Fig 5**). Ivermectin did not have significantly different EC_{10} results among the six strains, suggesting that natural variation in these strains does not affect ivermectin resistance. Moxidectin had undefined EC_{10} (estimates greater than the maximum exposure) and slope estimates, suggesting higher doses are needed to measure phenotypic responses across strains. Taken together, these results suggest that the genetic differences among *C. elegans* strains mediate differential susceptibilities across the majority of MLs.

To quantify the degree of phenotypic variation attributable to segregating genetic differences among strains, we estimated the H^2 and h^2 of the phenotypic responses in all MLs (**Fig 5C**). We observed that H^2 ranged from 0.02 in 0.00533 µM ivermectin to 0.87 in 0.27 µM milbemycin, and h^2 ranged from 0.01 in 0.00105 µM doramectin to 0.73 in 0.27 µM milbemycin. Heritability for moxidectin could not be calculated because modeling produced undefined EC_{10} and slope estimates (**Fig 4B**). In this strain set, we found milbemycin had the highest heritability

300 estimate, whereas ivermectin and selamectin had the lowest heritability estimates of the MLs,
301 indicating genetic variants between the six strains are involved in milbemycin response.

302 Another important factor in AR is suboptimal dosing of anthelmintics. Misdosing can cause
303 variability in how the drug reaches targeted nematodes and causes an insufficient anthelmintic
304 dose, which allows parasitic nematode populations to develop AR [45]. Although error-prone
305 dosing methods can impact AR across all drug classes, it may be particularly important for MLs
306 because small changes can cause vastly different anthelmintic responses. Here, we showed that
307 small changes in MLs doses can significantly vary in effectiveness because of the steep response
308 curves (**Fig 4**). Additionally, the bioavailability of an anthelmintic and the length of exposure time
309 also play a role in the dosage required to eliminate parasitic nematodes [46]. Correct dosing and
310 appropriate bioavailability are critical in all anthelmintic treatments, but this point is even more
311 striking in the MLs where the effective dose range is small.

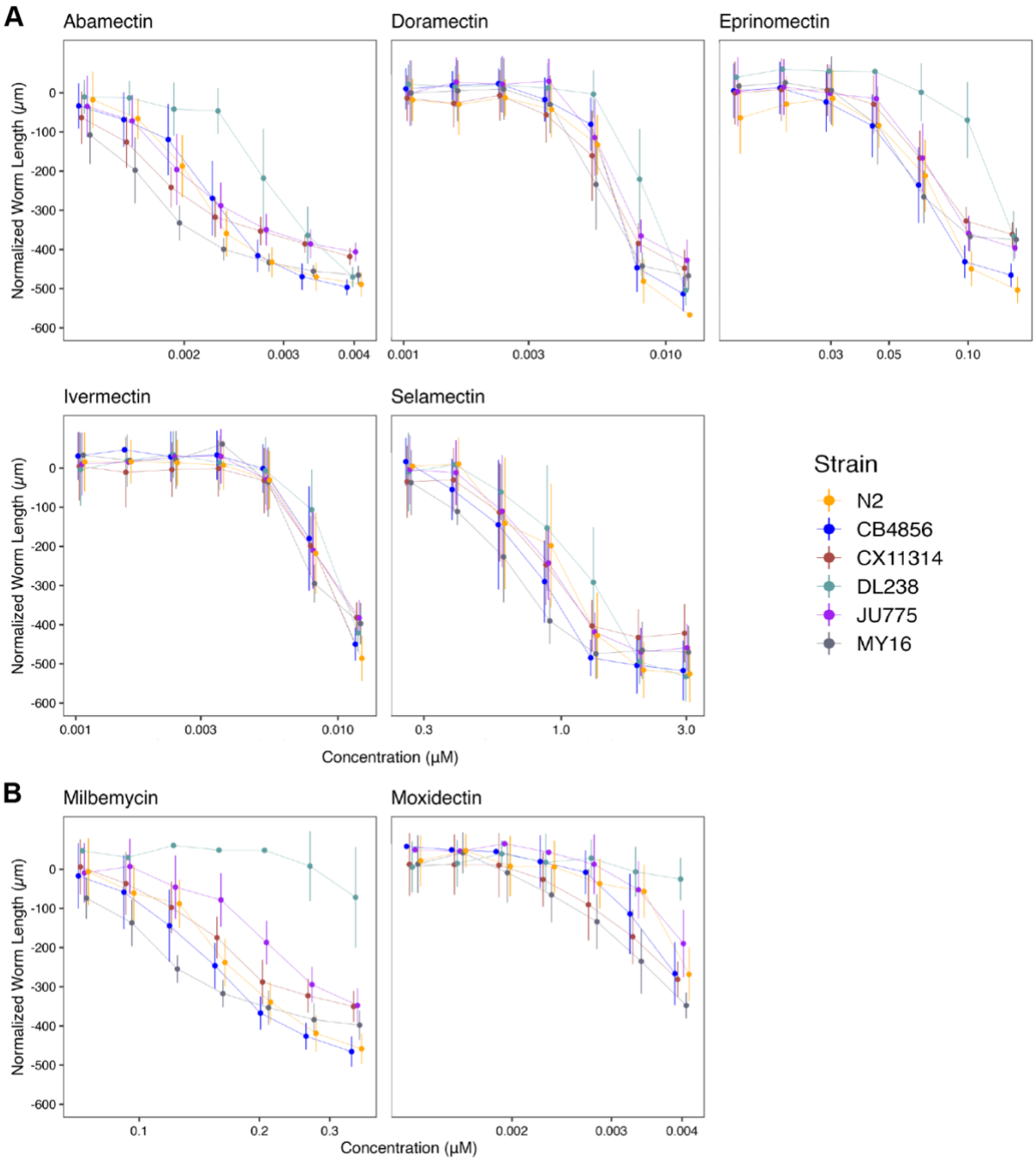

Figure 4. Dose-response curves for macrocyclic lactones (MLs). Normalized animal lengths (y-axis) are plotted for each strain as a function of the dose of macrocyclic lactone supplied in the high-throughput phenotyping assay (x-axis). Macrocyclic lactones are organized by **A)** Avermectins: Abamectin, Doramectin, Eprinomectin, Ivermectin, Selamectin; and **B)** Milbemycins: Milbemycin and Moxidectin. Strains are denoted by color. Lines extending vertically from points represent the standard deviation from the mean response. Statistical normalization of animal lengths is described in *Methods.*

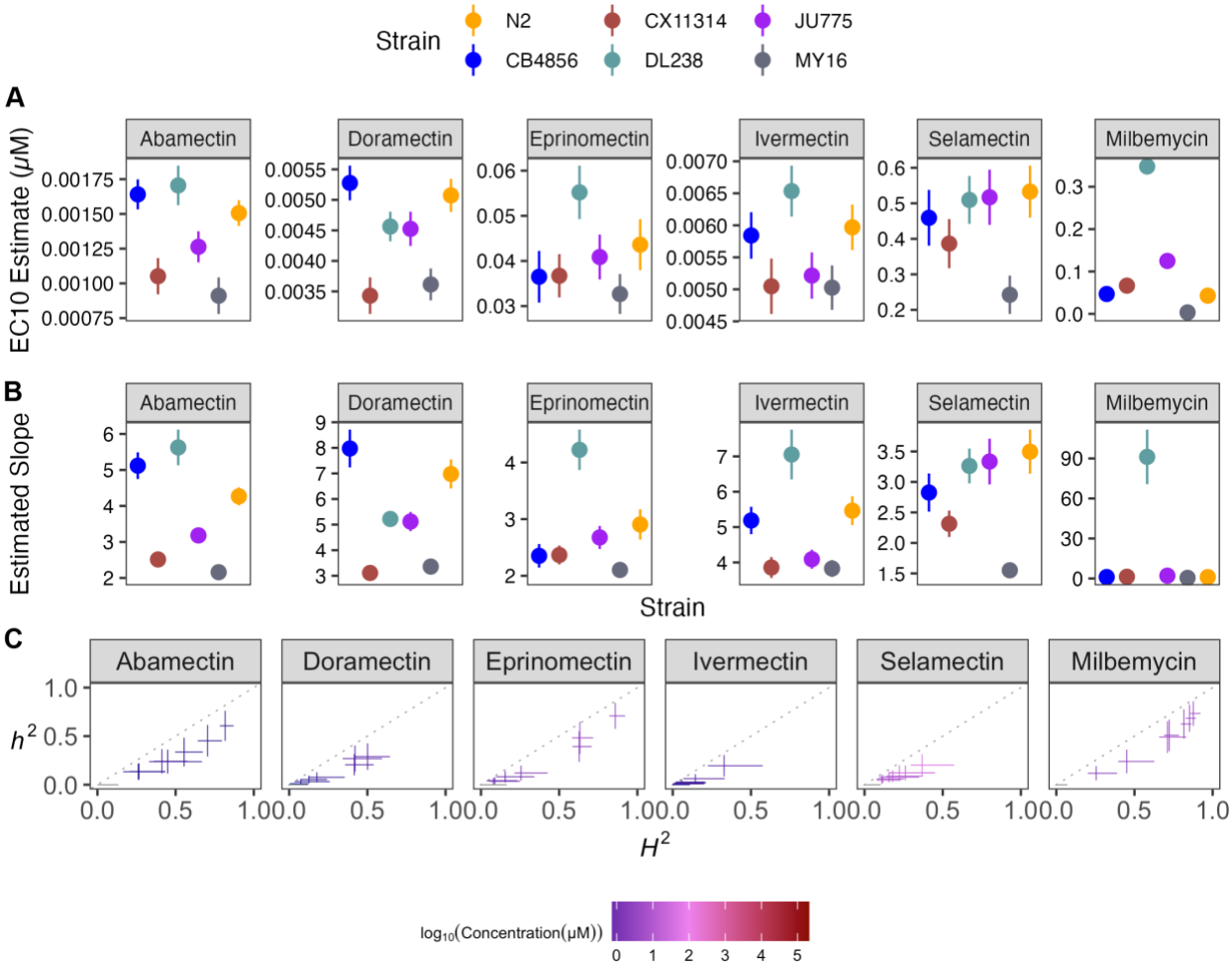

Figure 5. Variation in macrocyclic lactone (ML) EC_{10} dose-response and slope estimates can be explained by genetic variation across strains. A) Strain-specific EC_{10} estimates (*e*) for each macrocyclic lactone are displayed for each strain. Standard errors for each strain- and anthelmintic-specific EC_{10} estimates are indicated by the line extending vertically from each point. **B)** Strain-specific slope estimates (*b*) for each macrocyclic lactone are displayed for each strain. Standard errors for each strain- and anthelmintic-specific slope estimate are indicated by the line extending vertically from each point. **C)** The broad-sense (x-axis) and narrow-sense heritability (y-axis) of normalized animal length measurements were calculated for each concentration of each macrocyclic lactone (*Methods*; *Broad-sense and narrow-sense heritability calculations*). The color of each cross corresponds to the log-transformed dose for which those calculations were performed. The horizontal line of the cross corresponds to the confidence interval of the broad-sense heritability estimate obtained by bootstrapping, and the vertical line of the cross corresponds to the standard error of the narrow-sense heritability estimate. EC10, estimated slope, and heritability could not be calculated for moxidectin and, therefore, not plotted.

Natural genetic variation across *C. elegans* strains explains nAChR agonists responses

The nematode nAChRs in muscle cells are the target of the cholinergic agonists (*e.g.*, levamisole, pyrantel, and morantel [47]). These nAChR agonists cause ligand-gated ion channels to open, producing prolonged muscle contraction and spastic paralysis in nematodes [47]. Levamisole-sensitive nAChR subunits have been identified in the parasite *Ascaris summ* where three distinct pharmacological nAChR subtypes were present on muscle cells [48,49] and in *C. elegans* where mutations in the nAChR subunit genes *unc-29*, *unc-38*, *unc-63*, *lev-1*, and *lev-8* affect sensitivity [50–53].

Here, we assessed how natural variation contributes to phenotypic responses across three nAChR agonists composed of tetrahydropyrimidines (morantel and pyrantel) and an imidazothiazole (levamisole) (**S5 Table**, **Fig 6**). The nAChR agonists strain-specific slope (*b*) estimates for each dose-response model varied but followed near identical trends compared to EC_{10} estimates, indicating genetic variation is responsible for the observed response variation (**Fig 7**). The strain DL238 had the highest EC_{10} in levamisole. We found that the strain CB4856 had the highest EC_{10} for both tetrahydropyrimidines, whereas the CX11314 and MY16 strains had the lowest EC_{10} and are thus the most susceptible. Variable patterns across strains within the same drug class suggest nAChR agonists might be acting on different genetic targets.

EC_{10} and strain-specific slope (*b*) estimates suggested that the genetic differences among *C. elegans* strains mediate differential susceptibility across nAChR agonists. To quantify the degree of phenotypic variation attributable to segregating genetic differences among strains, we estimated the H^2 and h^2 of the phenotypic response for each dose of every nAChR agonist (**Fig 7C**). We observed that H^2 ranged from 0.06 in 300 µM pyrantel to 0.52 in 282.5 µM morantel, and h^2 ranged from 0.028 in 300 µM pyrantel to 0.34 in 82.5 µM morantel. We found morantel to elicit the most heritable response, whereas pyrantel elicited the lowest heritable response of the

nAChR agonists. Variable heritability in the tetrahydropyrimidines indicates that nAChR agonists may be acting on different genetic targets. Even if drugs have similar trends in EC_{10} and slope, heritability might help identify drugs where phenotypic variance in response to anthelmintic treatment is attributable to genetic differences. Additionally, although we have several genetic targets identified in *C. elegans*, it is unclear whether nAChR gene families remain highly conserved among nematode species or whether different species-specific functions can be exploited as potential targets for the control of particular parasites [54].

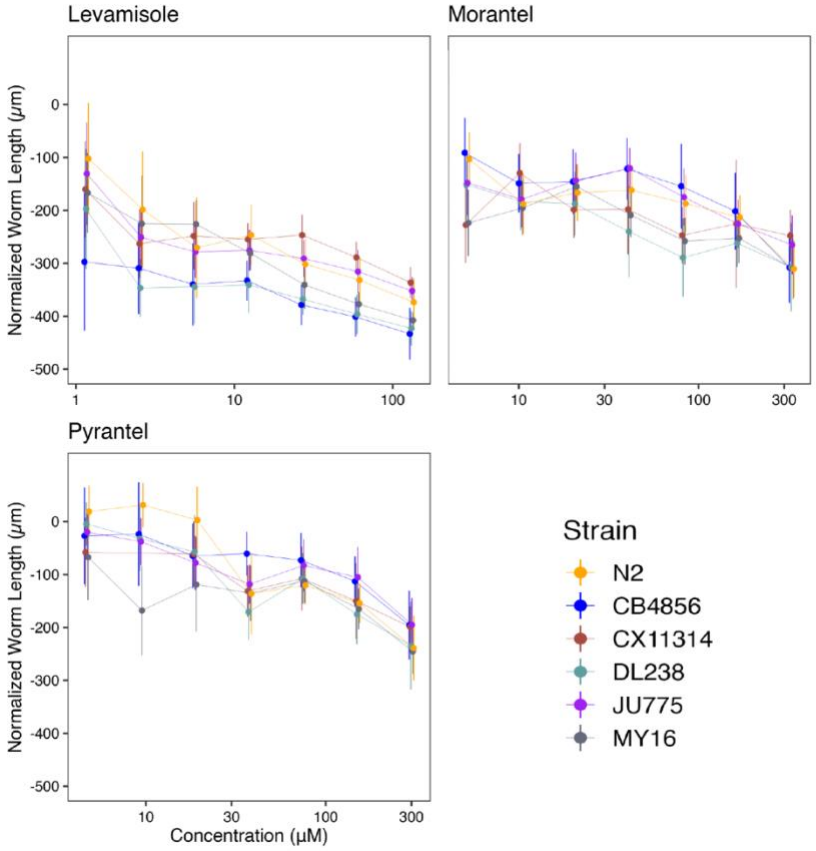

Figure 6. Dose-response curves for nicotinic acetylcholine receptor (nAChR) agonists. Normalized animal lengths (y-axis) are plotted for each strain as a function of the dose of anthelmintic supplied in the high-throughput phenotyping assay (x-axis); Levamisole, Morantel, and Pyrantel. Strains are denoted by color. Lines extending vertically from points represent the standard deviation from the mean response. Statistical normalization of animal lengths is described in *Methods.*

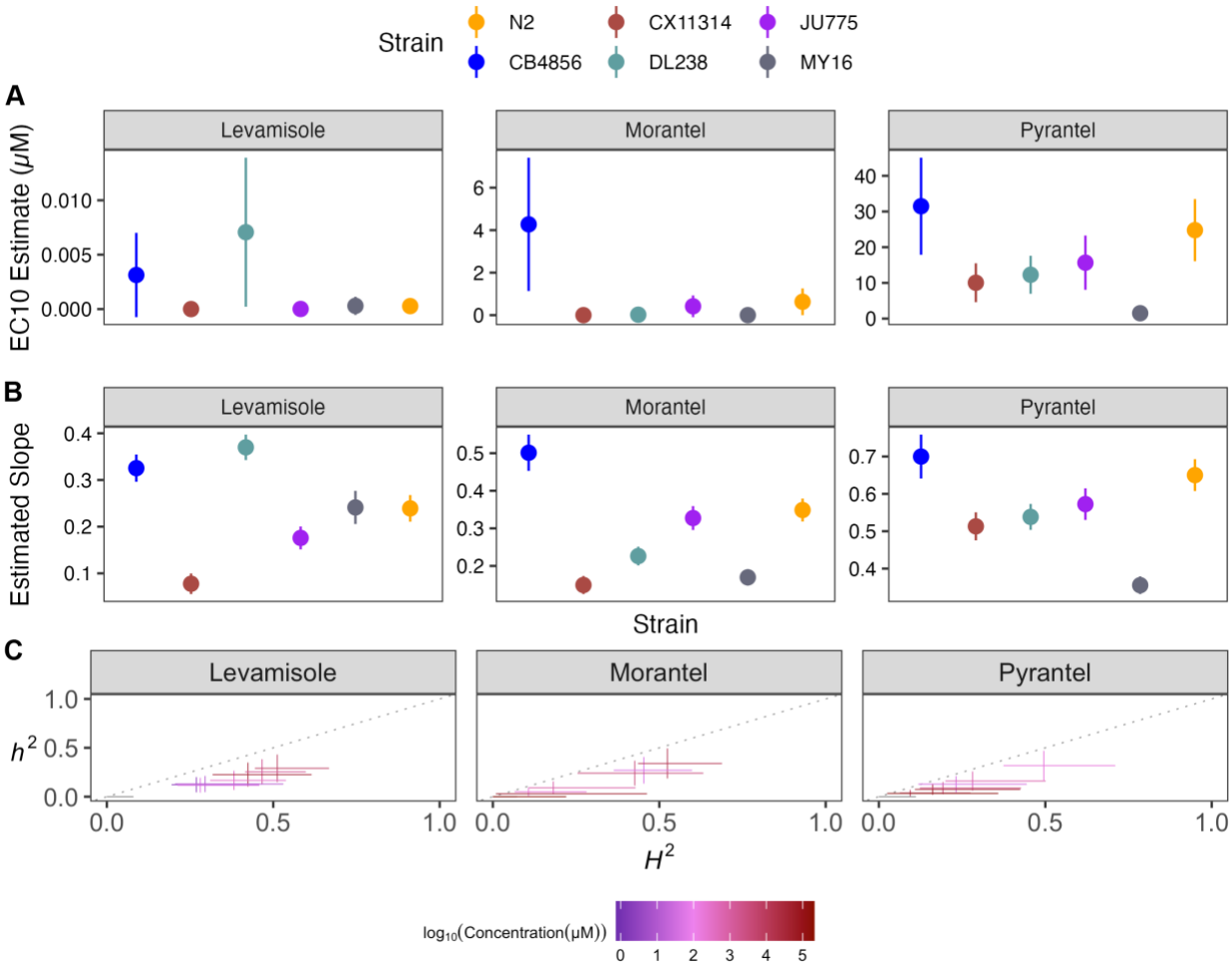

Figure 7. Variation in nicotinic acetylcholine receptor agonists (nAChR agonists) EC_{10} dose-response and slope estimates can be explained by genetic variation across strains. **A)** Strain-specific EC_{10} estimates (*e*) for each nicotinic acetylcholine receptor agonist are displayed for each strain. Standard errors for each strain- and anthelmintic-specific EC_{10} estimates are indicated by the line extending vertically from each point. **B)** Strain-specific slope estimates (*b*) for each nicotinic acetylcholine receptor agonist are displayed for each strain. Standard errors for each strain- and anthelmintic-specific slope estimate are indicated by the line extending vertically from each point. **C)** The broad-sense (x-axis) and narrow-sense heritability (y-axis) of normalized animal length measurements were calculated for each concentration of each nicotinic acetylcholine receptor agonist (*Methods*; *Broad-sense and narrow-sense heritability calculations*). The color of each cross corresponds to the log-transformed dose for which those calculations were performed. The horizontal line of the cross corresponds to the confidence interval of the broad-sense heritability estimate obtained by bootstrapping, and the vertical line of the cross corresponds to the standard error of the narrow-sense heritability estimates.

Dose-response assessments can be used across genetically diverse strains to identify anticipated anthelmintic effectiveness in combination therapies

Drugs outside of the three major anthelmintic classes are valuable because they have different hypothesized targets and mechanisms of resistance that could be effective against nematodes resistant to other drug classes. Drugs with different mechanisms of resistance can be used in combination therapies with other anthelmintics to create a more effective treatment. Although each anthelmintic class has different molecular targets, it is not well understood how a strain resistant to one class responds to another class. Here, in addition to the three major anthelmintic classes, we exposed strains to five different groups of anthelmintics categorized by their hypothesized drug targets. Nematode growth responses were measured against nAChR antagonists (monepantel sulfone, monepantel sulfide, and derquantel), a pore-forming crystal toxin (Cry5B), a cyclicoctadepsipeptide (emodepside), schistosomicides (niridazole, oxamniquine, and praziquantel), a salicylanilide (closantel), diethylcarbamazine, and piperazine (**S3 - S13 Fig**). By assessing nematode response patterns to individual drugs, we can identify which drugs could be paired in combination therapies.

In the past few decades, Cry5B and the nAChR agonist (Levamisole) have been used in combination therapy as strains resistant to nAChR agonists were susceptible to Cry5B [55]. Here, we find that the CB4856, DL238, and MY16 strains were sensitive to Cry5B, whereas the CX11314 and JU775 strains were sensitive to levamisole (**Fig 8, S14 Fig, S15 Fig**). We observed different patterns of susceptibility (strain rank order) between levamisole and Cry5B, indicating that this combined therapy could be an effective drug combination. Another promising combination therapy is derquantel and abamectin [56,57]. Derquantel and abamectin have been used in combination to treat multi-drug resistant *Haemonchus contortus* [58,59]. However, studies have found monepantel to be more effective than the combined derquantel and abamectin

417 treatment, although monepantel resistance is also prevalent, further exaggerating resistance
418 issues in *H. contortus* [56,60,61]. Here, we observed that the strain MY16 was most sensitive to
419 abamectin, whereas the CB4856 and DL238 strains were most resistant. In derquantel, we found
420 that the strains JU775 and MY16 were the most sensitive. Comparatively, the strain JU775
421 showed significant sensitivity to the monepantel drugs (monepantel sulfone, monepantel sulfide)
422 (**S8 Fig, S9 Fig**). Here, patterns of susceptibility and resistance indicated that combination
423 therapy composed of derquantel and abamectin would be a more effective treatment than
424 monepantel alone. Lastly, emodepside has also been commercialized and approved for
425 anthelmintic treatments in companion animals in combination with praziquantel [62]. Here, we find
426 that emodepside had heritable responses (**S7 Fig, S16 Fig**) among genetically diverse
427 *C. elegans,* but praziquantel had no heritable responses (**S13 Fig**). Although we describe
428 anticipated anthelmintic effectiveness in combination therapies, we acknowledge that a limitation
429 of this study is the small number of strains used. Even though we used a genetically divergent
430 strain set, we have captured a fraction of the genetic variation across the *C. elegans* species.
431 Promising combination therapies can be tested using larger strain sets. Altogether, dose-
432 response assessments in *C. elegans* provide a useful platform to assess hypothesized
433 effectiveness of drugs that can be used together in combination therapies.

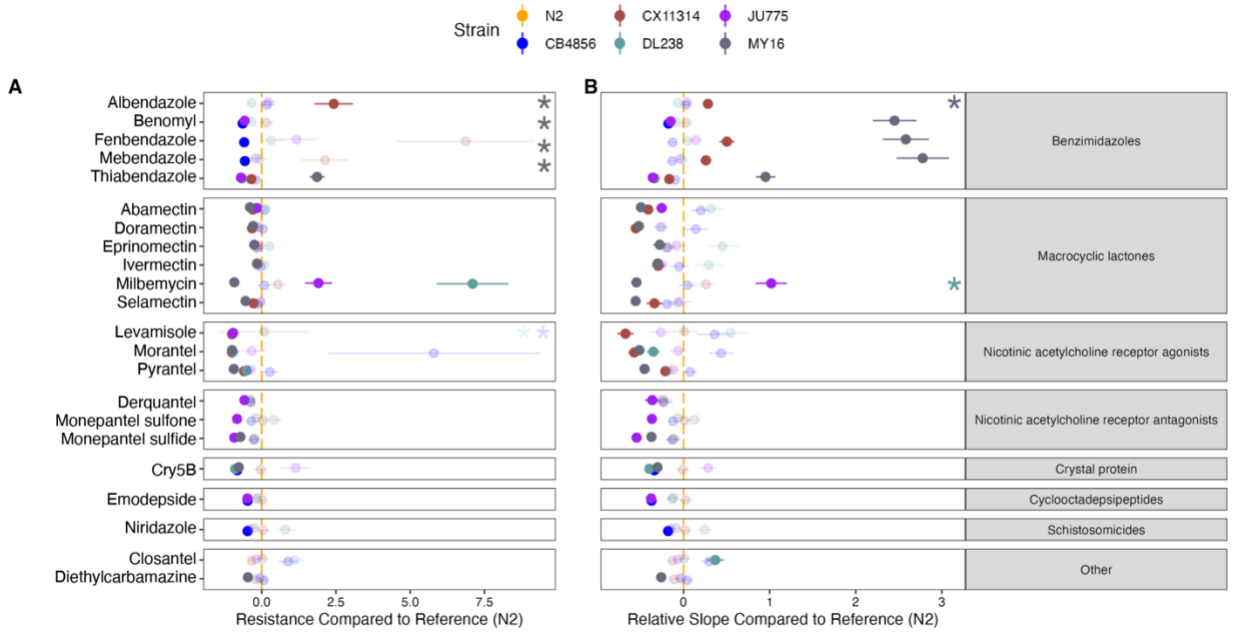

Figure 8. Variation in EC_{10} and dose-response slope estimates can be explained by genetic variation across strains. A) The relative potency of each anthelmintic for each strain compared to the N2 strain is shown. Solid points denote strains with significantly different relative resistance to that anthelmintic compared to the N2 strain (Student's t-test and subsequent Bonferroni correction with a $p_{adj} < 0.05$). Faded points denote strains not significantly different than the N2 strain. Asterisks denote strains with normalized estimates greater than ten compared to the N2 strain. See **Supplementary Figure 14** for the relative potency of all strains in each anthelmintic. Anthelmintic drugs with undefined EC_{10} estimates (estimates greater than the maximum dose to which animals were exposed) are not shown. **B)** For each anthelmintic, the relative steepness of the dose-response slope inferred for that strain compared to the N2 strain is shown. Solid points denote strains with significantly different dose-response slopes for that anthelmintic compared to the N2 strain (Student's t-test and subsequent Bonferroni correction with a $p_{adj} < 0.05$). Faded points denote strains without significantly different slopes than the N2 strain. Asterisks represent strains with slope estimates greater than 20 compared to the N2 strain. See **Supplementary Figure 15** for the slope estimates of all strains in each anthelmintic. Anthelmintic drugs with undefined slope estimates are not shown. The broad class to which each anthelmintic belongs is denoted by the strip label for each facet.

Dose-response assessment across genetically diverse stains identifies five anthelmintics for which *C. elegans* had little to no phenotypic responses

Because *C. elegans* is an inexpensive and highly tractable model, we could quickly assess which drugs we should continue to study in this model and drugs that will likely not provide useful results. Dose-response curves for the schistosomicides (niridazole, oxamniquine, and

praziquantel) showed little to no responses across *C. elegans* strains (**S10 Fig**, **S11 Fig**, **S13 Fig**). Minimal responses were also observed for diethylcarbamazine and piperazine (**S6 Fig**, **S12 Fig**). With minimal to no response for oxamniquine, praziquantel, and piperazine, EC_{10} and slope estimates could not be calculated. The schistosomicides have previously been shown to have no activity against nematodes [63], and thus it was not surprising that we observed little response in *C. elegans*. Diethylcarbamazine contains a piperazine ring that is essential for the activity of the drug and is the treatment of choice for lymphatic filariasis and loiasis [64]. Because piperazine did not cause a response in *C. elegans*, it is not surprising that diethylcarbamazine did not as well. Although little to no responses (*i.e.*, nematode growth defects) were observed for five drugs using our assays, it is possible assays measuring different fitness traits could elicit anthelmintic effects. Overall, *C. elegans* is a useful model for screening potential nematicides.

***C. elegans* is an invaluable model for understanding anthelmintic drug target identification and characterization**

Our assays measured *C. elegans* growth rates in the presence of anthelmintics across multiple concentrations of each drug, and this study yielded several major findings. First, dose-response experiments captured the variation in growth rate across six diverse strains within the *C. elegans* species. Growth trends yielded information that can be used to assess how other nematodes might respond to the tested anthelmintic drugs. Second, the large-scale HTA provided quantitative data with the required statistical power and sample sizes needed to effectively measure anthelmintic responses. Third, we were able to identify which drugs had heritable responses and, of those drugs, which doses were most heritable. The most heritable doses of each drug can be used in downstream GWAS to identify genomic regions correlated with AR [15]. By narrowing genomic intervals, subsequent candidate genes can be identified, edited, and

validated for anthelmintic responses to ultimately identify the genetic variants involved in resistance and inform downstream parasitic nematode treatments [33,36].

It is well established that parasitic nematodes are more genetically diverse than *C. elegans* and infect virtually all animal species, so understanding the role genetic diversity plays in anthelmintic resistance is critical [8]. The flow of resistance alleles within and among parasite populations has profound implications for the epidemiology of host infection, disease presentation, and the responses of parasite populations to selection pressures, such as anthelmintic treatment [5,65]. Additionally, the development of novel anthelmintics is slow, expensive, and complex, making it critical to correctly apply and monitor the usage of our existing drugs. We suggest that genetically diverse *C. elegans* strains should be deployed to aid high-throughput anthelmintic screening efforts to identify effective anthelmintics and estimated effective concentrations to use when testing in parasitic nematodes.

The presented data focused on the natural genetic variation in *C. elegans* and will require additional studies to identify genes responsible for the observed anthelmintic responses. This study summarized anthelmintic responses in naturally diverse *C. elegans* strains and highlighted drugs to focus on in downstream studies. Ultimately, AR gene variants responsible for observed effects need to be identified and validated in *C. elegans* and subsequently tested in parasitic nematodes.

MATERIALS AND METHODS

C. elegans strain selection and maintenance

Six *Caenorhabditis elegans* strains (CB4856, CX11314, DL238, JU775, MY16, PD1074) from the *C. elegans* Natural Diversity Resource (CeNDR) were used in this study [16]. Isolation details for the six strains are included in CeNDR. These strains were selected from the CeNDR divergent strain set, where the strain PD1074 is referred to by its isotype name, N2. In CeNDR,

strains that are >99.97% genetically identical are grouped into isotypes, PD1074 and N2 are nearly genetically identical, therefore, we chose to label PD1074 as N2 to illustrate the response of the canonical laboratory strain N2 [66]. Before measuring anthelmintic responses, animals were maintained at 20ºC on 6 cm plates with modified nematode growth medium (NGMA), which contains 1% agar and 0.7% agarose to prevent animals from burrowing. The NGMA plates were seeded with the *Escherichia coli* strain OP50 as a nematode food source. All strains were grown for three generations without starvation on the NGMA plates before anthelmintic exposure to reduce the transgenerational effects of starvation stress. The specific growth conditions for nematodes used in the high-throughput anthelmintic response assays are described below.

Nematode food preparation

Detailed nematode food preparation steps were followed as previously described [22]. One batch of HB101 *E. coli* was used as a nematode food source for all assays. Briefly, a frozen stock of HB101 *E. coli* was used to inoculate and grow a one-liter culture at an OD_{600} value of 0.001. A total of 14 cultures containing one liter of pre-warmed 1x Horvitz Super Broth (HSB) and an OD_{600} inoculum grew for 15 hours at 37ºC until cultures were in the late log growth phase. After 15 hours, flasks were removed from the incubator and transferred to 4ºC to arrest growth. Cultures went through three rounds of centrifugation, where the supernatant was removed, and the bacterial cells were pelleted. Bacterial cells were washed and resuspended in K medium. The OD_{600} value of the bacterial suspension was measured and diluted to a final concentration of OD_{600}100 with K medium, aliquoted to 15 ml conicals, and stored at -80ºC for use in the anthelmintic dose-response assays.

Anthelmintic stock preparation

All 26 anthelmintic stock solutions were prepared using either dimethyl sulfoxide (DMSO) or water, depending on the anthelmintic's solubility. Sources, catalog numbers, stock

concentrations, and preparation for each anthelmintic are provided (**S5 Table**). Anthelmintic stock solutions were prepared, aliquoted, and stored at -20ºC for use in the dose-response assays.

High-throughput anthelmintic dose-response assay

For each assay, populations of each strain were amplified and bleach-synchronized in triplicate. The bleach synchronization was replicated to control for variation in embryo survival and subsequent effects on developmental rates that could be attributed to bleach effects. After bleach synchronization, approximately 30 embryos were dispensed into the wells of a 96-well microplate in 50 µL of K medium. Strains were randomly assigned to columns of the 96-well microplates to vary strain column assignments across the replicate bleaches. Each strain was present in duplicate on each plate. Four replicate 96-well microplates within each of the three bleach replicates for each anthelmintic and control condition tested in the assay were prepared, labeled, and sealed using gas-permeable sealing films (Fisher Cat # 14-222-043). Plates were placed in humidity chambers to incubate overnight at 20ºC while shaking at 170 rpm (INFORS HT Multitron shaker). The following morning, food was prepared to feed the developmentally arrested first larval stage animals (L1s) using the required number of OD_{600}100 HB101 aliquots (see *Nematode food preparation*). The aliquots were thawed at room temperature, combined into a single conical tube, and diluted to an OD_{600}30 with K medium. To inhibit further bacterial growth and prevent contamination, 150 µM of Kanamycin was added to the HB101. Working with a single anthelmintic at a time, an aliquot of anthelmintic stock solution thawed at room temperature (see *Anthelmintic stock preparation*) and was diluted to a working concentration. The anthelmintic working concentration was set to the concentration that would give the highest desired dose when added to the 96-well microplates at 1% of the total well volume. The serial dilution of the anthelmintic working solution was prepared using the same diluent, DMSO or water, used to make the stock solution. The dilution factors ranged from 1.2 to 2.5 depending on the anthelmintic used, but all serial dilutions had eight concentrations, including a 0 µM control. The serial dilution was

then added to an aliquot of the OD_{600}30 K medium at a 3% volume/volume ratio. Next, 25 µl of the food and anthelmintic mixture was transferred into the appropriate wells of the 96-well microplates to feed the arrested L1s at a final HB101 concentration of OD_{600}10 and expose L1 larvae to an anthelmintic at one of eight levels of the dilution series. Immediately afterward, the 96-well microplates were sealed using a new gas permeable sealing film, returned to the humidity chambers, and incubated for 48 hours at 20ºC shaking at 170 rpm. The remaining 96-well microplates were fed and exposed to anthelmintics in the same manner. After 48 hours of incubation in the presence of food and anthelmintic, the 96-well microplates were removed from the incubator and treated with 50 mM sodium azide in M9 for 10 minutes to paralyze and straighten nematodes. Images of nematodes in the microplates were immediately captured using a Molecular Devices ImageXpress Nano microscope (Molecular Devices, San Jose, CA) using a 2X objective. The ImageXpress Nano microscope acquires brightfield images using a 4.7 megapixel CMOS camera and stores images in a 16-bit TIFF format. The images were used to quantify the development of nematodes in the presence of anthelmintics as described below (see *Data collection* and *Data cleaning*).

Data processing

CellProfiler software (Version 4.0.3) was used to quantify animal lengths from images collected on the Molecular Devices ImageXpress Nano microscope (Carpenter et al. 2006). A Nextflow pipeline (Version 20.01.0) was written to run command-line instances of CellProfiler in parallel on the Quest High-Performance Computing Cluster (Northwestern University). The CellProfiler workflow can be found at (https://github.com/AndersenLab/cellprofiler-nf). CellProfiler modules and Worm Toolbox were developed to extract morphological features of individual *C. elegans* animals from images from the HTA [67]. The custom CellProfiler pipeline generates animal measurements by using four worm models: three worm models tailored to capture animals at the L4 larval stage, in the L2 and L3 larval stages, and the L1 larval stage, respectively, as well

as a “multi-drug high dose” (MDHD) model, to capture animals with more abnormal body sizes caused by extreme anthelmintic responses. Worm model estimates and custom CellProfiler pipelines were written using the WormToolbox in the GUI-based instance of CellProfiler [23]. Next, a custom R package, *easyXpress* (Version 1.0), was then used to process animal measurements output from CellProfiler [17]. These measurements comprised our raw dataset.

Data Cleaning

The presented analysis has been modified from previous work [22]. All analyses were performed using the R statistical environment (version 4.2.1) unless stated otherwise. The high-throughout anthelmintic dose-response assay produced thousands of images per experimental block; thus, we implemented a systematic approach to assess the quality of animal measurement data in each well. Several steps were implemented to clean the raw image data using metrics indicative of high-quality animal measurements for downstream analysis.

1) Objects with a *Worm_Length* > 30 pixels, 100 microns, were removed from the CellProfiler data to (A) retain L1 and MDHD-sized animals and (B) remove unwanted particles [68]. Using the *Worm_Length* > 30 pixels threshold to retain small sensitive animals, more small objects, such as debris, were also retained (see *Supplementary Information*).
2) *R/easyXpress* [17] was used to filter measurements from worm objects within individual wells with statistical outliers and to parse measurements from multiple worm models down to single measurements for single animals.
3) The data were visualized by drug, drug concentration, assay, strain, and worm model for two purposes. First, to ensure that each drug, by assay, contained control wells that had a *mean_wormlength_um* between 600 - 800 µm, the size of an L4 animal. If the *mean_wormlength_um* in the control wells was not between the 600 - 800 µm range, then that strain and/or assay were removed for the drug

(**S17 Fig**). This filter ensured the control wells, DMSO or water, primarily contained L4 animals. Assays and drugs that did not meet the control well *mean_wormlength_um* criteria and were thus subsequently removed were: abamectin (assay A), derquantel (assay H), niridazole (assay H), eprinomectin (assay I), and piperazine (assay I). Second, we wanted to identify drugs that contained a high abundance of MDHD model objects across all assays and drug concentrations. Drugs with an abundance of objects classified by the MDHD model across assays and concentrations likely contain debris. The MDHD model was removed from the following 13 drugs to limit debris and small objects: albendazole, benomyl, Cry5B, diethylcarbamazine, fenbendazole, mebendazole, morantel, niridazole, oxamniquine, piperazine, praziquantel, pyrantel, and thiabendazole.

4) We then filtered the data to wells containing between three and forty animals, under the null hypothesis that the number of animals is an approximation of the expected number of embryos originally titered into wells (approximately 30). Given that our analysis relied on well median animal length measurements, we excluded wells with less than three animals to reduce sampling error.
5) We removed statistical outlier measurements within each concentration for each strain for every anthelmintic drug to reduce the likelihood that statistical outliers influence anthelmintic dose-response curve fits.
6) Next, we removed measurements from all doses of each anthelmintic drug that were no longer represented in at least 80% of the independent assays because of previous data filtering steps.
7) Finally, we normalized the data by (1) regressing variation attributable to assay and technical replicate effects and (2) normalizing these extracted residual values to the average control phenotype. For each anthelmintic drug, we estimated a

linear model using the raw phenotype measurement as the response variable, and both assay and technical replicate identity as explanatory variables following the formula *median_wormlength_um ~ Metadata_Experiment + bleach* using the *lm()* function in base R. We used the residuals from the linear model to remove the effect of assay and bleach from the raw phenotypes. Next, for each drug, we calculated the mean of residual values in control conditions for each strain in each assay and bleach. Finally, for each drug, strain, assay, and bleach, we subtracted the appropriate mean control values from the model residuals to arrive at our normalized length measurements, which were used in all downstream statistical analyses. These normalized length measurements have the helpful property of being centered on zero in control conditions for each strain and, therefore, control for natural differences in the length of the strains.

Small object removal and data cleaning

In previous analyses, we used *Worm_Length > 50* (165 microns) to filter out small objects from data before performing cleaning steps [22]. For the anthelmintics, we saw that when applying this filter, high dose concentrations for 12 of the 26 anthelmintics were filtered and removed. Additionally, the anthelmintic selamectin was entirely removed from the dataset (**S18 Fig**). Although a *Worm_Length > 50* filtered debris from image data, it also filtered small drug-affected nematodes, which were abundant in this study. To ensure that we captured small drug-affected nematodes across anthelmintics and minimized the amount of retained debris, we altered the animal length threshold to *Worm_Length > 30* (100 microns). The threshold *Worm_Length > 30* was previously recorded as the smallest animal length of L1 animals after an hour of feeding [68]. To confirm that we were retaining animal objects, we (1) retained the MDHD model for drugs that had small animals present at high dose concentrations (see *Methods* and *Data Cleaning*) and (2) observed high dose well images to ensure the MDHD model was identifying nematodes.

Dose-response model estimation and statistics

Dose-response model estimates and statistics have been modified from previous work [22]. We estimated overall and strain-specific dose-response models for each anthelmintic by fitting a log-logistic regression model using *R/drc* (Version 3.0.1) [69]. The four-parameter log-logistic function, *LL.4*, fit the anthelmintic data best. The *LL.4* model was fit to each anthelmintic using the *drc::drm()* function, where the model specified the following parameters: *b*, the slope of the dose-response curve; *c*, the upper asymptote of the dose-response curve; *d*, the lower asymptote of the dose-response curve; and e, the effective dose [70]. Strain was specified as a covariate for parameters *b* and *e*, allowing us to estimate strain-specific dose-response slopes and effective doses. The lower asymptote, *d*, was specified at -600, the theoretical normalized length of animals at the first larval stage.

The *drc::ED()* function was used to extract strain-specific EC_{10} values and strain-specific slope values were extracted. We quantified the relative susceptibilities of each strain pair for each compound based on their estimated EC_{10} values using the *drc::EDcomp()* function, which used an approximate *F*-test to determine whether the variances (represented by delta-specified confidence intervals) calculated for each strain-specific dose-response model's *e* parameter estimates were significantly different. We quantified the relative slope steepness of dose-response models estimated for each strain within each compound using the *drc::compParm()* function, which used a *z*-test to compare the means of each *b* parameter estimate. Results shown were filtered to comparisons against N2 dose-response parameters (**Fig 8**), and significantly different estimates in both cases were determined by correcting to a family-wise type I error rate of 0.05 using a Bonferroni correction. To determine whether strains were significantly more resistant or susceptible to more anthelmintics or anthelmintic classes by chance, we conducted 1000 Fisher exact tests using the *fisher.test()* function with 2000 Monte Carlo simulations.

Broad-sense and narrow-sense heritability calculations

Broad-sense heritability was estimated (H^2) using in the R statistical environment (version 4.0.4) using the R package, *lme4* (v1.1-27.1) to fit a linear mixed-effects model to the normalized median animal length data using strain as a random effect. H^2 was calculated using the equation, $H^2 = V_G / (V_G+V_E)$, where we extracted the among strain variance (V_G) and residual variance (V_E). Genetic variance (V_G) can be partitioned into additive (V_A) and non-additive (V_{NA}) variance components.

Narrow-sense heritability (h^2) measures the additive genetic variance over the total phenotypic variance, $h^2 = V_A / V_P$. To calculate h^2, we first generated a strain matrix using the strain *genomatrix profile* on NemaScan, a genome-wide association (GWA) mapping and simulation pipeline [71], using the variant call format (VCF) file generated in the 20220216 CeNDR release (https://www.elegansvariation.org/data/release/latest). We then calculated h^2 using the *sommer* (v4.1.3) R package by calculating the variance-covariance matrix (M_A) from the strain matrix using the *sommer::A.mat* function. We estimated V_A using the linear mixed-effects model function *sommer::mmer* using strain as a random effect and M_A as the covariance matrix. We then estimated h^2 and its standard error using the *sommer::vpredict* function (**S16 Fig**).

Data availability

All code and data used to replicate the data analysis and figures are available at https://github.com/AndersenLab/anthelmintic_dose_responses_manuscript and Zenodo DOI: 10.5281/zenodo.7351693.

AUTHOR CONTRIBUTIONS

Conceptualization: Erik C. Andersen, Janneke Wit

Data Curation: Amanda O. Shaver

Formal Analysis: Amanda O. Shaver

Funding Acquisition: Erik C. Andersen

706 **Investigation:** Janneke Wit

707 **Methodology:** Janneke Wit, Clayton M. Dilks

708 **Project Administration:** Erik C. Andersen

709 **Resources:** Erik C. Andersen, Hanchen Li, Raffi V. Aroian

710 **Software:** Amanda O. Shaver, Timothy A. Crombie

711 **Supervision:** Erik C. Andersen

712 **Validation:** Amanda O. Shaver, Timothy A. Crombie

713 **Visualization:** Amanda O. Shaver

714 **Writing - Original Draft Preparation:** Amanda O. Shaver

715 **Writing - Review & Editing:** Amanda O. Shaver, Janneke Wit, Clayton M. Dilks, Timothy A.

716 Crombie, Erik C. Andersen

717

718 **ACKNOWLEDGMENTS**

719 We would like to thank members of the Andersen laboratory for their feedback and helpful

720 comments on this manuscript. We thank the *C. elegans* Natural Diversity Resource (NSF

721 Capacity grant 2224885) for providing us with strains for this study. We thank Joy N. Nyaanga,

722 Timothy A. Crombie, and Samuel J. Widmayer for creating *easyXpress*, a critical software tool

723 used in this study. We thank Samuel J. Widmayer and Timothy A. Crombie for sharing the toxicant

724 dose-response code and workflow used in this study. We thank the following people for providing

725 us with the following drugs: Troy Hawkins for monepantel sulfone LY33414916 and monepantel

726 sulfide LY3348298, and Daniel Kulke for emodepside.

REFERENCES

1. de Silva NR, Brooker S, Hotez PJ, Montresor A, Engels D, Savioli L. Soil-transmitted helminth infections: updating the global picture. Trends Parasitol. 2003;19: 547–551.

2. Dieterich, Sommer. How to become a parasite–lessons from the genomes of nematodes. Trends Genet. Available: https://www.sciencedirect.com/science/article/pii/S016895250900064X

3. Kotze AC, Gilleard JS, Doyle SR, Prichard RK. Challenges and opportunities for the adoption of molecular diagnostics for anthelmintic resistance. Int J Forecast. 2020. Available: https://www.sciencedirect.com/science/article/pii/S2211320720300476

4. Sangster NC, Cowling A, Woodgate RG. Ten events that defined anthelmintic resistance research. Trends Parasitol. 2018. Available: https://www.sciencedirect.com/science/article/pii/S1471492218300941

5. Hodgkinson JE, Kaplan RM, Kenyon F, Morgan ER, Park AW, Paterson S, et al. Refugia and anthelmintic resistance: Concepts and challenges. International Journal for Parasitology: Drugs and Drug Resistance. 2019. pp. 51–57. doi:10.1016/j.ijpddr.2019.05.001

6. James CE, Hudson AL, Davey MW. Drug resistance mechanisms in helminths: is it survival of the fittest? Trends Parasitol. 2009;25: 328–335.

7. Hahnel, Dilks, Heisler, Andersen. Caenorhabditis elegans in anthelmintic research–Old model, new perspectives. Int J Educ Vocat Guid. 2020. Available: https://www.sciencedirect.com/science/article/pii/S2211320720300312

8. Hahnel SR, Dilks CM, Heisler I, Andersen EC, Kulke D. Caenorhabditis elegans in anthelmintic research – Old model, new perspectives. International Journal for Parasitology: Drugs and Drug Resistance. 2020. pp. 237–248. doi:10.1016/j.ijpddr.2020.09.005

9. Dilks CM, Hahnel SR, Sheng Q, Long L, McGrath PT, Andersen EC. Quantitative benzimidazole resistance and fitness effects of parasitic nematode beta-tubulin alleles. Int J Parasitol Drugs Drug Resist. 2020;14: 28–36.

10. Dilks CM, Koury EJ, Buchanan CM, Andersen EC. Newly identified parasitic nematode beta-tubulin alleles confer resistance to benzimidazoles. Int J Parasitol Drugs Drug Resist. 2021;17: 168–175.

11. Wit J, Dilks CM, Andersen EC. Complementary Approaches with Free-living and Parasitic Nematodes to Understanding Anthelmintic Resistance. Trends Parasitol. 2021;37: 240–250.

12. Kwok TCY, Ricker N, Fraser R, Chan AW, Burns A, Stanley EF, et al. A small-molecule screen in C. elegans yields a new calcium channel antagonist. Nature. 2006;441: 91–95.

13. Leung CK, Wang Y, Malany S, Deonarine A, Nguyen K, Vasile S, et al. An ultra high-throughput, whole-animal screen for small molecule modulators of a specific genetic pathway in Caenorhabditis elegans. PLoS One. 2013;8: e62166.

14. Lemieux GA, Liu J, Mayer N, Bainton RJ, Ashrafi K, Werb Z. A whole-organism screen identifies new regulators of fat storage. Nat Chem Biol. 2011;7: 206–213.

15. Evans KS, van Wijk MH, McGrath PT, Andersen EC, Sterken MG. From QTL to gene: C. elegans facilitates discoveries of the genetic mechanisms underlying natural variation. Trends Genet. 2021;37: 933–947.

16. Cook DE, Zdraljevic S, Roberts JP, Andersen EC. CeNDR, the Caenorhabditis elegans natural diversity resource. Nucleic Acids Res. 2017;45: D650–D657.

17. Nyaanga J, Crombie TA, Widmayer SJ, Andersen EC. easyXpress: An R package to analyze and visualize high-throughput C. elegans microscopy data generated using CellProfiler. PLoS One. 2021;16: e0252000.

18. Hahnel SR, Zdraljevic S, Rodriguez BC, Zhao Y, McGrath PT, Andersen EC. Extreme allelic heterogeneity at a Caenorhabditis elegans beta-tubulin locus explains natural resistance to benzimidazoles. PLoS Pathog. 2018;14: e1007226.

19. Evans KS, Andersen EC. The Gene scb-1 Underlies Variation in Caenorhabditis elegans Chemotherapeutic Responses. G3 . 2020;10: 2353–2364.

20. Wit J, Rodriguez BC, Andersen EC. Natural variation in Caenorhabditis elegans responses to the anthelmintic emodepside. Int J Parasitol Drugs Drug Resist. 2021;16: 1–8.

21. Brady SC, Zdraljevic S, Bisaga KW, Tanny RE, Cook DE, Lee D, et al. A Novel Gene Underlies Bleomycin-Response Variation in Caenorhabditis elegans. Genetics. 2019;212: 1453–1468.

22. Widmayer SJ, Crombie TA, Nyaanga JN, Evans KS, Andersen EC. C. elegans toxicant responses vary among genetically diverse individuals. Toxicology. 2022; 153292.

23. Widmayer SJ, Crombie TA, Nyaanga J, Evans KS, Andersen EC. *C. elegans* toxicant responses vary among genetically diverse individuals. doi:10.1101/2022.07.19.500602

24. Theodorides VJ, Scott GC, Lademan MS. Strains of Haemonchus contortus resistant against benzimidazole anthelmintics. Am J Vet Res. 1970;31: 859–863.

25. Roos MH, Kwa MSG, Grant WN. New genetic and practical implications of selection for anthelmintic resistance in parasitic nematodes. Parasitol Today. 1995;11: 148–150.

26. Kotze AC, Hunt PW, Skuce P, von Samson-Himmelstjerna G, Martin RJ, Sager H, et al. Recent advances in candidate-gene and whole-genome approaches to the discovery of anthelmintic resistance markers and the description of drug/receptor interactions. Int J Parasitol Drugs Drug Resist. 2014;4: 164–184.

27. Driscoll M, Dean E, Reilly E, Bergholz E, Chalfie M. Genetic and molecular analysis of a Caenorhabditis elegans beta-tubulin that conveys benzimidazole sensitivity. J Cell Biol. 1989;109: 2993–3003.

28. Lubega GW, Prichard RK. Specific interaction of benzimidazole anthelmintics with tubulin: high-affinity binding and benzimidazole resistance in Haemonchus contortus. Mol Biochem Parasitol. 1990;38: 221–232.

29. Kwa MS, Veenstra JG, Roos MH. Benzimidazole resistance in Haemonchus contortus is correlated with a conserved mutation at amino acid 200 in beta-tubulin isotype 1. Mol Biochem Parasitol. 1994;63: 299–303.

30. Vercruysse J, Behnke JM, Albonico M, Ame SM, Angebault C, Bethony JM, et al. Assessment of the anthelmintic efficacy of albendazole in school children in seven countries where soil-transmitted helminths are endemic. PLoS Negl Trop Dis. 2011;5: e948.

31. Keiser J, Utzinger J. Efficacy of current drugs against soil-transmitted helminth infections: systematic review and meta-analysis. JAMA. 2008;299: 1937–1948.

32. Levecke B, Montresor A, Albonico M, Ame SM, Behnke JM, Bethony JM, et al. Assessment of anthelmintic efficacy of mebendazole in school children in six countries where soil-transmitted helminths are endemic. PLoS Negl Trop Dis. 2014;8: e3204.

33. Zamanian M, Cook DE, Zdraljevic S, Brady SC, Lee D, Lee J, et al. Discovery of genomic intervals that underlie nematode responses to benzimidazoles. PLoS Negl Trop Dis. 2018;12: e0006368.

34. Latheef SLJ. The use of natural genetic variation in Caenorhabditis elegans to identify novel polymorphisms that can confer benzimidazole resistance in nematodes. Graduate Studies; 2014. doi:10.11575/PRISM/28412

35. Doyle SR, Laing R, Bartley D, Morrison A, Holroyd N, Maitland K, et al. Genomic landscape of drug response reveals novel mediators of anthelmintic resistance. bioRxiv. 2022. p. 2021.11.12.465712. doi:10.1101/2021.11.12.465712

36. Evans KS, Wit J, Stevens L, Hahnel SR, Rodriguez B, Park G, et al. Two novel loci underlie natural differences in Caenorhabditis elegans abamectin responses. PLoS Pathog. 2021;17: e1009297.

37. Prichard RK, Geary TG. Perspectives on the utility of moxidectin for the control of parasitic nematodes in the face of developing anthelmintic resistance. Int J Parasitol Drugs Drug Resist. 2019;10: 69–83.

38. Dent JA, Smith MM, Vassilatis DK, Avery L. The genetics of ivermectin resistance in Caenorhabditis elegans. Proc Natl Acad Sci U S A. 2000;97: 2674–2679.

39. Page AP. The sensory amphidial structures of Caenorhabditis elegans are involved in macrocyclic lactone uptake and anthelmintic resistance. Int J Parasitol. 2018;48: 1035–1042.

40. Rezansoff AM, Laing R, Gilleard JS. Evidence from two independent backcross experiments supports genetic linkage of microsatellite Hcms8a20, but not other candidate loci, to a major ivermectin resistance locus in Haemonchus contortus. Int J Parasitol. 2016;46: 653–661.

41. Doyle SR, Illingworth CJR, Laing R, Bartley DJ, Redman E, Martinelli A, et al. Population genomic and evolutionary modelling analyses reveal a single major QTL for ivermectin drug resistance in the pathogenic nematode, Haemonchus contortus. BMC Genomics. 2019;20: 218.

42. Choi Y-J, Bisset SA, Doyle SR, Hallsworth-Pepin K, Martin J, Grant WN, et al. Genomic introgression mapping of field-derived multiple-anthelmintic resistance in Teladorsagia circumcincta. PLoS Genet. 2017;13: e1006857.

43. Stear MJ, Boag B, Cattadori I, Murphy L. Genetic variation in resistance to mixed, predominantly Teladorsagia circumcincta nematode infections of sheep: from heritabilities to gene identification. Parasite Immunol. 2009;31: 274–282.

44. Doyle SR, Bourguinat C, Nana-Djeunga HC, Kengne-Ouafo JA, Pion SDS, Bopda J, et al. Genome-wide analysis of ivermectin response by Onchocerca volvulus reveals that genetic drift and soft selective sweeps contribute to loss of drug sensitivity. PLoS Negl Trop Dis. 2017;11: e0005816.

45. Vercruysse J, Levecke B, Prichard R. Human soil-transmitted helminths: implications of mass drug administration. Curr Opin Infect Dis. 2012;25: 703–708.

46. Lanusse C, Canton C, Virkel G, Alvarez L, Costa-Junior L, Lifschitz A. Strategies to Optimize the Efficacy of Anthelmintic Drugs in Ruminants. Trends Parasitol. 2018;34: 664–682.

47. Harrow ID, Gration KAF. Mode of action of the anthelmintics morantel, pyrantel and levamisole on muscle cell membrane of the nematodeAscaris suum. Pestic Sci. 1985;16: 662–672.

48. Levandoski MM, Robertson AP, Kuiper S, Qian H, Martin RJ. Single-channel properties of N- and L-subtypes of acetylcholine receptor in Ascaris suum. International Journal for Parasitology. 2005. pp. 925–934. doi:10.1016/j.ijpara.2005.03.007

49. Pharmacology of N-, L-, and B-subtypes of nematode nAChR resolved at the single-channel level in Ascaris suum. The FASEB Journal. 2006;20: 2606–2608.

50. Lewis JA, Wu CH, Berg H, Levine JH. The genetics of levamisole resistance in the nematode Caenorhabditis elegans. Genetics. 1980;95: 905–928.

51. Culetto E, Baylis HA, Richmond JE, Jones AK, Fleming JT, Squire MD, et al. The Caenorhabditis elegans unc-63 Gene Encodes a Levamisole-sensitive Nicotinic Acetylcholine Receptor α Subunit*. J Biol Chem. 2004;279: 42476–42483.

52. Fleming JT, Squire MD, Barnes TM, Tornoe C, Matsuda K, Ahnn J, et al. Caenorhabditis elegans Levamisole Resistance Geneslev-1, unc-29, and unc-38 Encode Functional Nicotinic Acetylcholine Receptor Subunits. J Neurosci. 1997;17: 5843–5857.

53. Towers PR, Edwards B, Richmond JE, Sattelle DB. The Caenorhabditis elegans lev-8 gene encodes a novel type of nicotinic acetylcholine receptor alpha subunit. J Neurochem. 2005;93: 1–9.

54. Brown LA, Jones AK, Buckingham SD, Mee CJ, Sattelle DB. Contributions from Caenorhabditis elegans functional genetics to antiparasitic drug target identification and validation: Nicotinic acetylcholine receptors, a case study. Int J Parasitol. 2006;36: 617–624.

55. Hu Y, Platzer EG, Bellier A, Aroian RV. Discovery of a highly synergistic anthelmintic combination that shows mutual hypersusceptibility. Proc Natl Acad Sci U S A. 2010;107: 5955–5960.

56. Kaminsky R, Bapst B, Stein PA, Strehlau GA, Allan BA, Hosking BC, et al. Differences in efficacy of monepantel, derquantel and abamectin against multi-resistant nematodes of sheep. Parasitol Res. 2011;109: 19–23.

57. Epe C, Kaminsky R. New advancement in anthelmintic drugs in veterinary medicine. Trends Parasitol. 2013;29: 129–134.

58. Sager H, Bapst B, Strehlau GA, Kaminsky R. Efficacy of monepantel, derquantel and abamectin against adult stages of a multi-resistant Haemonchus contortus isolate. Parasitol Res. 2012;111: 2205–2207.

59. Woods DJ, Maeder SJ, Robertson AP, Martin RJ, Geary TG, Thompson DP, et al. Discovery, mode of action, and commercialization of derquantel. Parasitic Helminths. Weinheim, Germany: Wiley-VCH Verlag GmbH & Co. KGaA; 2012. pp. 297–307.

60. Mederos AE, Ramos Z, Banchero GE. First report of monepantel Haemonchus contortus resistance on sheep farms in Uruguay. Parasit Vectors. 2014;7: 598.

61. Van den Brom R, Moll L, Kappert C, Vellema P. Haemonchus contortus resistance to monepantel in sheep. Veterinary Parasitology. 2015. pp. 278–280. doi:10.1016/j.vetpar.2015.02.026

62. Altreuther G, Buch J, Charles SD, Davis WL, Krieger KJ, Radeloff I. Field evaluation of the efficacy and safety of emodepside/praziquantel spot–on solution against naturally acquired nematode and cestode

infections in domestic cats. Parasitol Res. 2005;97: S58–S64.

63. Holden-Dye L, Walker R. Anthelmintic drugs and nematocides: studies in Caenorhabditis elegans. Maricq AV, editor. WormBook. 2014; 1–29.

64. Bennett MD MACP J, Dolin R, Blaser MJ. Mandell, Douglas, and Bennett's Principles and Practice of Infectious Diseases: 2-Volume Set. Elsevier Health Sciences; 2014.

65. Kaplan RM. Drug resistance in nematodes of veterinary importance: a status report. Trends Parasitol. 2004;20: 477–481.

66. Yoshimura J, Ichikawa K, Shoura MJ, Artiles KL, Gabdank I, Wahba L, et al. Recompleting the Caenorhabditis elegans genome. Genome Res. 2019;29: 1009–1022.

67. Wählby C, Kamentsky L, Liu ZH, Riklin-Raviv T, Conery AL, O'Rourke EJ, et al. An image analysis toolbox for high-throughput C. elegans assays. Nat Methods. 2012;9: 714–716.

68. Nyaanga J, Andersen EC. Linkage mapping reveals loci that underlie differences in C. elegans growth. G3 . 2022. doi:10.1093/g3journal/jkac207

69. Ritz C, Jensen SM, Gerhard D, Streibig JC. Dose-Response Analysis Using R. CRC Press; 2019.

70. Seber GAF, Wild CJ. Nonlinear Regression. Wiley Series in Probability and Statistics. 1989. doi:10.1002/0471725315

71. Widmayer, Evans, Zdraljevic. Evaluating the power and limitations of genome-wide association studies in C. elegans. G3 Genes| Genomes. doi:10.1093/g3journal/jkac114/6583190